Accepted Manuscript

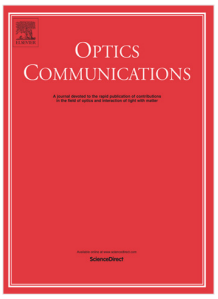

The theory of selective reflection for a Fabry–Perot interferometer

Davit N. Khachatryan

PII: S0030-4018(18)31043-5
DOI: https://doi.org/10.1016/j.optcom.2018.11.078
Reference: OPTICS 23663

To appear in: *Optics Communications*

Received date : 26 October 2018
Revised date : 27 November 2018
Accepted date : 28 November 2018

Please cite this article as: D.N. Khachatryan, The theory of selective reflection for a Fabry–Perot interferometer, *Optics Communications* (2018), https://doi.org/10.1016/j.optcom.2018.11.078

The theory of selective reflection for a Fabry-Perot interferometer

Davit N. Khachatryan

Institute for Physical Research, NAS of Armenia, Ashtarak-2, 0203 Armenia

Abstract

In this paper we revisit the theory of selective reflection from a dilute vapor cell. A self-consistent theory is developed for reflection spectrum for Fabry-Perot interferometer. Formulas for single and multiple reflections are obtained. We also obtain the effective refractive index for a single selective reflection. The results of the paper are in a good agreement with existing experimental results.

Keywords: Laser spectroscopy, Reflection and refraction, Line shapes, widths, and shifts, Interference
PACS: 42.62.Fi, 42.25.Gy, 32.70.Jz, 42.25.Hz

1. Introduction

Reflection of radiation from the boundary between a dielectric and atomic vapor, when laser field is detuned in the vicinity of atomic transition frequencies, is termed selective reflection (SR) [1–3]. SR has many applications, such as locking a diode laser frequency to atomic resonance lines [4–6], retrieval of group refractive index [7], marking atomic transition resonance lines [8, 9], study of the van der Waals interaction of atoms with a dielectric surface [10–12], determination of the homogeneous width and the shift of resonance lines [12–15] and cross-sections of resonant collisions [16], study of coherent and magneto-optical processes [17–22].

Since many decades, and until now, the theory of SR is investigated by many authors [3, 23–30]. Schuurmans in his paper [3] developed a theory,

Email address: khachatryan.ipr@gmail.com (Davit N. Khachatryan)

where he obtained the spectral narrowing of a SR signal. In [24] a theory of frequency modulated SR was developed, that allows one to obtain Doppler free spectral lines. The problem of different frequency shifts existing in a SR signal was discussed by [25–27] (e.g. caused by local field correction, atom-wall interaction and etc.) while in [28–30] theories are developed for the dilute thin vapor cells.

The sub-Doppler reflection spectrum in a SR signal is due to atom-wall collisions. After a collision atoms leave the wall in the ground state. This creates a spatial transient region, where the polarization has dependence on the spatial coordinate. The existence of this transient region was experimentally demonstrated by several authors [31, 32] by using evanescent wave fluorescence spectrum from the atoms that are near the dielectric wall.

In [33] it was shown that by changing the thickness of the cell's sapphire window with highly parallel surfaces one can change the SR signal shape, because of the Fabry-Perot interferometer effect. Also, one can change the SR signal shape by changing the length of the thin (nanometric) vapor cell [9]. In the present paper we will demonstrate that the SR line shape can be changed also for a thicker (cm order) cell.

The present paper is an extension of the theoretical model discussed in [7]. We develop a self-consistent theory by using the density matrix formalism. In the calculations we use Laplace transformation that let us obtain formulas for single and multiple selective reflections. Also, the effective complex refractive index for a single selective reflection was obtained. We assume that after atom-wall collisions all atoms lose their polarization [28, 30]. Since light is directed normally to the cell boundary, it is enough to consider a one-dimensional problem.

In the next section, after recalling elements of our study concerning the reflection from a Fabry–Perot interferometer by taking into account the steady-state solution, then we will take into account the transient behavior of polarization of a dilute vapor cell. We obtain new formulas for single and multiple reflection spectra and discuss the considered approximations. Additionally, we will compare the new formulas with the classical ones. In section 4 we will present the effective refractive index and discuss its properties. In the last section we compare our results with existing experimental ones.

2. Basic concepts

In this section we are going to focus mainly on basic concepts and classical formulas in order to compare them with our obtained results. Firstly, we recall the interaction properties between light and a vapor modeled by a two-level system. The cell consists of three layers (glass, vapor, glass). All boundaries are parallel to each other and light is directed normally to the first boundary. The magnetic field is set to zero and the cw laser field is assumed to be weak enough to neglect the associated nonlinear effects.

We describe light-medium interactions by Maxwell equations using the Liouville-von Neumann density matrix formalism,

$$\begin{aligned} &\frac{d^2E}{dx^2} + k^2E = -4\pi k^2 P, \\ &\frac{d\rho}{dt} = -\frac{i}{\hbar}[\mathcal{H}, \rho] + \Lambda, \\ &P = NTr(\rho d), \end{aligned} \tag{1}$$

where E is the amplitude of the electric field, P is the polarization of the medium, N is the density of atoms, d is the dipole moment of resonant atoms, $\mathcal{H}$ is the Hamiltonian of the system, and Λ is the dissipation matrix, which describes all the relaxation processes, as well as the laser radiation linewidth. In the presence of spatial dispersion, P also is a function of the spatial coordinate x. This case will be discussed in the next section.

The continuity of the electromagnetic field at the borders $x = 0$ and $x = L$ of the medium reads

$$\begin{aligned} &E(0) = E_I + E_R, \\ &E'(0) = ikn_1(E_I - E_R), \\ &E(L) = E_T, \\ &E'(L) = ikn_2E_T, \end{aligned} \tag{2}$$

where E_I is the amplitude of the incident light, E_R is the amplitude of the reflected light, E_T is the amplitude of the transmitted light, $n_{1,2}$ are the refractive indexes of the windows, $k = \omega/c$ is the wave vector, ω is the frequency of the field and c is the speed of light in vacuum.

The ρ_{21} density matrix component of the two-level system in the linear approximation obeys the equation

$$u\frac{\partial \rho_{21}}{\partial x} = i\Omega e^{-i(\omega t-\varphi)} - (\Gamma + i\omega_0)\rho_{21}, \tag{3}$$

where $\Omega = \frac{|E||d|}{\hbar}$ is the Rabi frequency, $\Gamma = \gamma/2+\Gamma_l+\Gamma_c+...$ is the transverse decay rate, γ is the natural decay rate of the excited state, Γ_l is the laser spectral width, Γ_c is a phenomenological decay rate that models the collisions, u is the velocity of atoms, ω_0 is the resonant frequency and φ is the phase of the field.

For a very dense vapor, we can assume that the nomogeneous width $\Gamma \gg ku_T$, where ku_T is the Doppler width and u_T is the most probable thermal velocity of atoms. Therefore, the $u\frac{\partial \rho_{21}}{\partial x}$ term in (3) can be neglected [28]. So, from equations (1), (3) one obtains classical formulas for susceptibility χ and refractive index n

$$\begin{aligned} \chi &= \frac{iq}{\Gamma - i\Delta}, \\ n &= \sqrt{1+4\pi\chi}, \end{aligned} \tag{4}$$

where $\Delta = \omega - \omega_0$ is the detuning from the resonance frequency ω_0, $q = \frac{N|d|^2}{\hbar}$ is a parameter of the medium.

From (1), (2) and (4) one obtains the well known formulas for the field within media

$$\begin{aligned} E(x) &= E_I A e^{-iknx} + E_I B e^{iknx}, \\ A &= \frac{\widetilde{R} - r_1}{2n(n_1+n)}, \\ B &= \frac{1-\widetilde{R}r_1}{2n(n_1+n)}, \end{aligned} \tag{5}$$

with the Fabry-Perot interferometer reflection coefficients

$$\begin{aligned} \widetilde{R} &= \frac{r_1 - r_2 e^{2iknL}}{1 - r_1 r_2 e^{2iknL}}, \\ r_{1,2} &= \frac{n_{1,2} - n}{n_{1,2} + n}, \end{aligned} \tag{6}$$

where $R = \left|\widetilde{R}\right|^2$ is the reflection coefficient for the Fabry-Perot interferometer. If we set $n_1 = n_2 = n_0$ (and, therefore, $r_1 = r_2 = r$), we find the classic formula for R:

$$R = \left| \frac{r - re^{2iknL}}{1 - r^2 e^{2iknL}} \right|^2. \tag{7}$$

The formulas presented in (6) and (7) are well known from classical theory of the Fabry-Perot interferometer [34]. For a more rigorous solution of (3) one should not neglect $u\frac{\partial \rho_{21}}{\partial x}$ and find a solution that takes into account the transient behavior of the medium. This problem will be solved in the next section. It will allow to compare the approximate solution (7) with rigorous one.

3. Spatial Dispersion

We assume now that the atoms lose their polarization after atom-wall collisions, thus leave the wall in the ground state. Taking this in account, the boundary conditions for the medium polarization (see for example [28, 30]):

$$P(x = 0, u > 0) = 0, \qquad P(x = L, u < 0) = 0. \tag{8}$$

From equations (1) and (8) one can derive

$$P(x) = \int_0^x E(y)\langle \chi(x - y)\rangle_{u>0} dy + \int_L^x E(y)\langle \chi(x - y)\rangle_{u<0} dy, \tag{9}$$

where $\chi(x) = \frac{iq}{u} e^{-\frac{-i\Delta}{u}x}$ is the linear susceptibility for the medium with a spatial dispersion and $\langle\ \rangle_u$ denotes averaging over velocities supposed to verify a Maxwellian distribution. Note that when $x > L$ then $P(x) = 0$ $(N = 0)$.

We dont need to solve (1) with the polarization (9) because it is sufficient to find only the asymptotic solution when $x \to L$. Obviously, the second integral vanishes when $x \to L$. It results the differential equation

$$\frac{d^2 E(x)}{dx^2} + k^2 E(x) = -4\pi k^2 \int_0^x E(y)\langle \chi(x - y)\rangle_{u>0} dy. \tag{10}$$

Denoting $\widetilde{\chi}(s)$ and $\widetilde{E}(s)$ the Laplace transforms of $\langle \chi(x - y)\rangle_{u>0}$ and $E(x)$, equation (10) leads to

$$\widetilde{E}(s) = \frac{sE(0) + E'(0)}{s^2 + k^2(1 + 4\pi\widetilde{\chi}(s))}, \tag{11}$$

$$\widetilde{\chi}(s) = \langle \frac{iq}{\Gamma + su - i\Delta} \rangle_{u>0}, \tag{12}$$

where we have used the property of the Laplace transformation from the convolution of object functions.

Here we will do the following approximation. We will assume that the denominator of (11) admit two roots s_1 and s_2 thus

$$s^2 + k^2(1 + 4\pi\widetilde{\chi}(s)) = (s - s_1)(s - s_2), \tag{13}$$

where s_1 and s_2 are given by the following iteration procedure ($s_1^{(0)}$ and $s_2^{(0)}$ are the roots of denominator of (11) when $\chi(s) = 0$)

$$\begin{aligned} s_1^{(0)} &= -ik, \qquad s_2^{(0)} = ik, \\ s_1^{(n)} &= -ik(1 + 2\pi\widetilde{\chi}(s_1^{(n-1)})) = -ikn(s_1^{(n-1)}), \\ s_2^{(n)} &= ik(1 + 2\pi\widetilde{\chi}(s_2^{(n-1)}))) = ikn(s_2^{(n-1)}), \end{aligned} \tag{14}$$

here n is the iteration step. At each step of iteration we will obtain more precise values for $s_{1,2}$. The procedure converges when $4\pi\left|\widetilde{\chi}(s_{1,2})\right| \ll 1$ and gives the approximate roots of the denominator of (11). The convergence of the iteration procedure is demonstrated in Fig.1.

From Fig.1 one can see that only three iterations are needed in order to find s_1 and s_2. We should note that for densities $N > 10^{15}\text{cm}^{-3}$ the iteration procedure doesn't work, because $4\pi\left|\widetilde{\chi}(s_{1,2})\right| \ll 1$ relation is not true for these densities. The dependence of $4\pi\left|\widetilde{\chi}(s_{1,2}))\right|$ on the density of atoms is shown in Fig.2.

With the expression (13), we can rewrite (11) as follows:

$$\widetilde{E}(s) = \frac{sE(0) + E'(0)}{(s - s_1)(s - s_2)}. \tag{15}$$

Inverse Laplace transformation leads to:

$$E(x) = \frac{s_1E(0) + E'(0)}{s_1 - s_2}e^{s_1x} - \frac{s_2E(0) + E'(0)}{s_1 - s_2}e^{s_2x}. \tag{16}$$

Here we should remember that (16) is an approximative solution, hence, it is correct only for $x \to L$. With the use of (16), we get $E(L)$ and $E'(L)$:

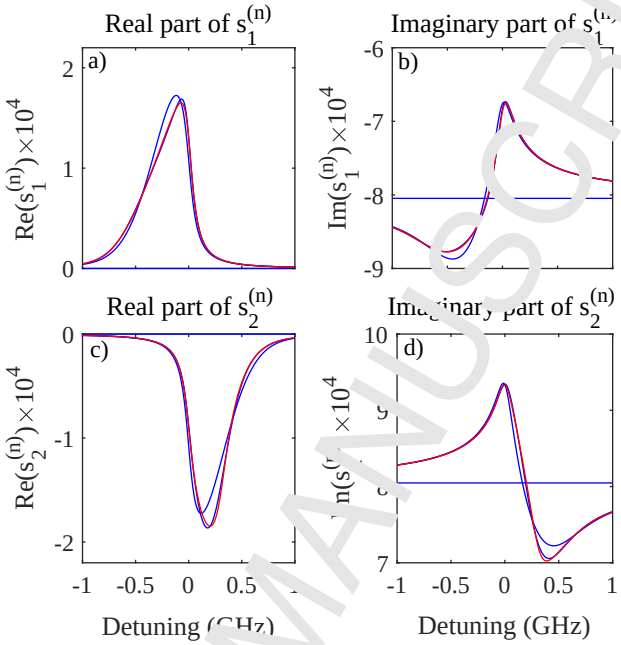

Figure 1: The convergence of the iteration procedure. a) and b) correspond to real and imaginary parts of s_1 and c) and d) correspond to real and imaginary parts of s_2. In all four plots the red solid lines correspond to 10th iteration from (14), blue solid horizontal lines correspond to $n = 0$ iteration step, and the rest blue solid lines correspond to $n = 1, 2$ iterations. The density of atoms is $N = 10^{15}\mathrm{cm}^{-3}$ and $\Gamma_c = 2\pi \cdot 53\mathrm{MHz}$.

$$
\begin{aligned}
E(L) &= \frac{s_1 E(0) + E'(0)}{s_1 - s_2} e^{s_1 L} - \frac{s_2 E(0) + E'(0)}{s_1 - s_2} e^{s_2 L}, \\
E'(L) &= \frac{s_1^2 E(0) + s_1 E'(0)}{s_1 - s_2} e^{s_1 L} - \frac{s_2^2 E(0) + s_2 E'(0)}{s_1 - s_2} e^{s_2 L}.
\end{aligned}
\tag{17}
$$

From (17) together with the conditions from (2), one deduces an expression for $\tilde{\Sigma} = E_R/E_I$:

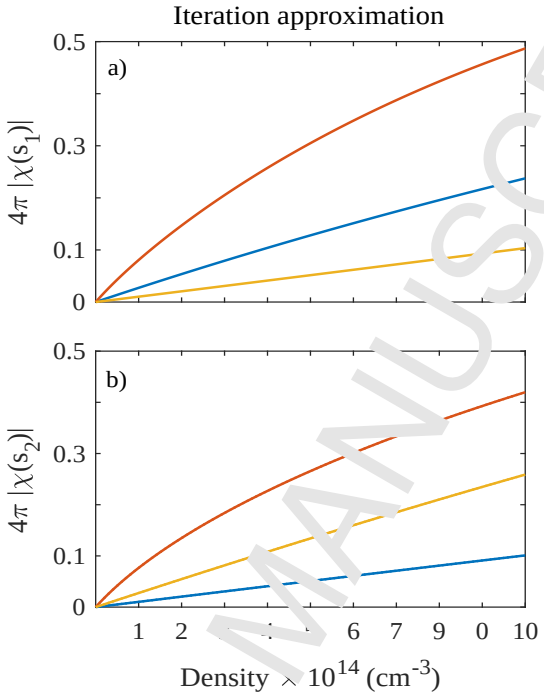

Figure 2: Dependence of $4\pi|\widetilde{\chi}(s_k)|$ (where $k = 1, 2$ corresponds respectfully to sub-figures a) and b) on the density of atoms. The red lines correspond to $\Delta = 0$, the yellow lines to $\Delta = 0.5$GHz and the blue ones to $\Delta = -0.5$GHz.

$$\begin{aligned}
\widetilde{R} &= \frac{r_1(s_1) - Dr_2(s_2)e^{\phi}}{1 - Dr_1(s_2)r_2(s_2)e^{\phi}}, \\
D &= \frac{(n_1 + n(s_2))(n_2 + n(s_2)}{(n_1 + n(s_1))(n_2 + n(s_1))}, \\
r_l(s_m) &= \frac{n_l - n(s_m)}{n_l + n(s_m)}, \\
\phi &= 2ikn_{avg}L,
\end{aligned} \tag{18}$$

where $l, m = 1, 2$ are integers and $n_{avg} = (n(s_1) + n(s_2))/2$.

In (18) one can notice two exponential expressions, one of which is increasing ($Re(s_1) > 0$) and the other one is decreasing ($Re(s_2) < 0$), when $x \to \infty$. So, a natural question arises: when $L \to \infty$ and, consequently, x

can increase to infinity, can the first term become infinite? If so, this solution will be non physical (the field should be zero at infinity). To show that there is no problem with the first term, we rewrite (16) by using the conditions from (2) in the following way:

$$\begin{aligned} E(x) &= E_I A e^{s_1 x} + E_I B e^{s_2 x}, \\ A &= \frac{\widetilde{R} - r_1(s_1)}{(n(s_1)+n(s_2))(n_1 + n(s_1))} \\ B &= \frac{1 - \widetilde{R} r_1(s_2)}{(n(s_1)+n(s_2))(n_1 + n(s_2))}. \end{aligned} \tag{19}$$

By substituting the expression of $\widetilde{R}$ from (18) into the first term of (19) we obtain the behavior

$$E_I A e^{s_1 x} \propto e^{L - s_1(L-x)}. \tag{20}$$

From (20) one notices that when $L \to \infty$ it tends to zero for every $x \in (0, L)$. So, when we have only the first border (or the second border is far enough) we can neglect the exponentially increasing term in (19). Therefore, there are no problems with infinities.

If we set $n_1 = n_2 = n_0$ in the expression for $\widetilde{R}$ from (18) we get a more simpler expression for the reflection coefficient $R = \left|\widetilde{R}\right|^2$:

$$R = \left| \frac{r(s_1) - D r(s_2) e^{\phi}}{1 - D r^2(s_2) e^{\phi}} \right|^2. \tag{21}$$

In the next section we compare this result with the classical formula (7) and we discuss physical meaning of $n(s_1)$ and n_{avg}. Note that all our previous calculations do not imply any restriction on the length, thus equation (21) can be used for higher thicknesses than those discussed in [28–30] (see, Fig.8 here after).

4. Effective refractive index

Dissipative atom collisions with the wall create a transient spatial region near the boundaries of the cell. In this transient region we do not have one uniform vapor, thus, we can not describe our medium with a "simple" linear refractive index [35]. From (9) one observes nonlocal dependence of the

polarization on the spatial coordinate x. Thus, the refractive index should depend on x. Although, it is difficult to derive the expression of the refractive index for this kind of medium, we are able to attribute the concept of effective refractive index to the medium.

First of all, let us compare our formula (21) with the classical formula (7) for the reflection coefficient. In (21), instead of r we have $r(s_1)$ and $r(s_2)$ and we have an additional term D. D like all other terms of (21) have a dependence on the detuning Δ, but D is always close to one and can be neglected. Notice that the refractive index n in (7) and n_{avg} from (21) appear both in the phase of exponents in the corresponding formulas. So, n_{avg} in (21) plays the same role as n in (7). This comparison can lead to an assumption that n_{avg} can play the role of the refractive index in our medium. The real and imaginary parts of n_{avg} are presented in Fig.3.

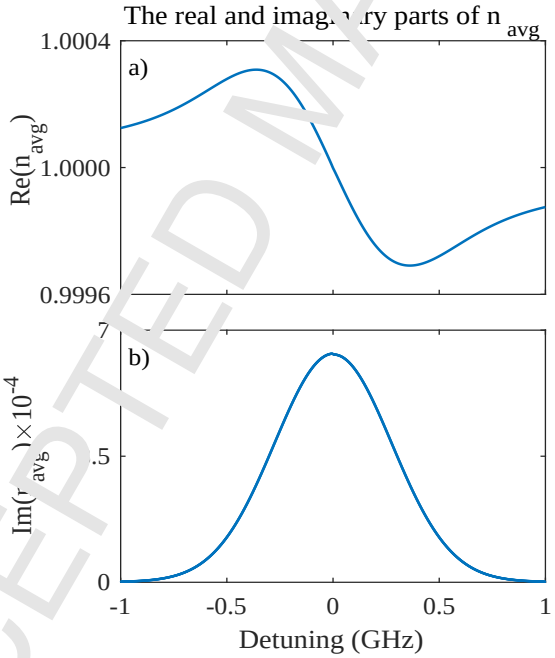

Figure 3: The spectra of a) real and b) imaginary parts of n_{avg}. The density of atoms is $N = 1 \cdot 10^{12}$ cm^{-3}.

As one can see from Fig.3, the curve of the real part of n_{avg} has an dispersive profile and the curve of the imaginary part of n_{avg} has a absorptive profile, like the refractive index in the conventional theory [36]. This is

another argument that n_{avg} has the physical meaning of the refractive index inside the medium.

From (21) we can derive another interesting relation, if we assume that the cell is long enough ($L \to \infty$). Notice that $e^{\phi} \to 0$, when $L \to \infty$ ($Im(n_{avg}) > 0$) and we deduce the following formula:

$$R_s = \left|r(s_1)\right|^2 = \left|\frac{n_0 - n(s_1)}{n_0 + n(s_1)}\right|^2. \tag{22}$$

In this relation only the first reflection from the cell is taken into account, thus, it represents the formula for the single reflective reflection. Notice that (22) is similar to the Fresnel equation for normal incidence. Therefore, we can say that $n(s_1)$ plays the role of the refractive index. So, we will call $n(s_1)$ the effective complex refractive index for a single reflection. Also, by analogy to the Fresnel equation, we will attribute $Im(n(s_1))$ as the effective absorption, and $Re(n(s_1))$ as the effective real refractive index. Moreover, $n(s_1)$ can also be referred to as the surface admittance $M = E'(0)/(ikE(0))$ as defined in [3]. In Fig.4 we show the dependence of $Im(n(s_1))$ and $Re(n(s_1))$ on the detuning from the resonance line.

In the effective absorption curve in Fig.4*b* one can see that the absorption curve is red-shifted. This means that the atoms with positive velocities have dominant contribution in the absorption curve. It is interesting to recall the experimental results obtained by Burgmans et al. [31], where the authors observed fluorescence radiation from the transient region of the Na vapor. They showed that the spectrum of fluorescence of atoms near the wall has a decrease in the blue-shifted sides of resonance lines. The reason is the possibility for the atoms being polarized and moving towards the boundary to lose their polarization non-radiatively by quenching to the wall. In Fig.4 one can notice that the effective absorption curve is different from the absorption curve described by the conventional theory [36]. The difference, like in [31] experiment, is in the blue-shifted side from the resonance line. So, in this sense, we can claim that our result is consistent with that experiment. The steep drop of the line in the effective absorption profile is due to the conditions given by (9), where we stated in first approximation that all atoms after collision lose their polarization non-radiatively.

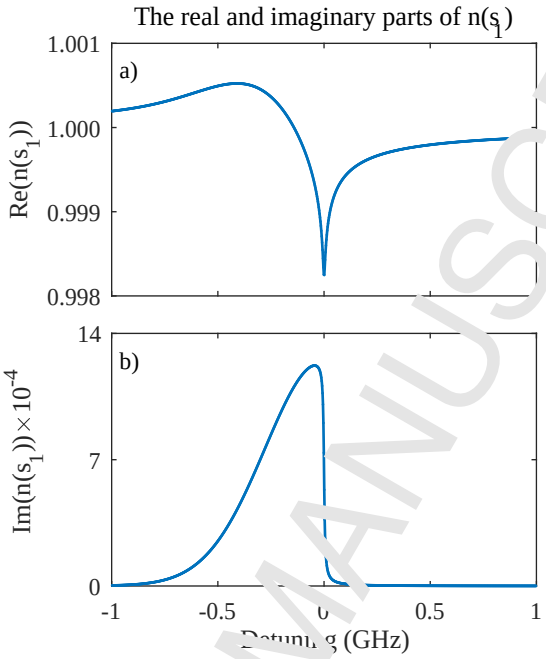

Figure 4: The spectra for a) the effective real refractive index and b) the effective absorption. The density of atoms is $N = 4 \cdot 10^{12}\mathrm{cm}^{-3}$.

5. Selective reflection

In Fig.5 we show the dispersion of the single selective reflection calculated from (22).

The result presented in Fig.5 is similar to the well known profile of the selective reflection (for instance, see Fig. 8 in [37]). Of course, it is a rough simplification to assume that we have only a single resonance line. In real experiments multilevel systems are considered. Thus if one wants to generalize to multilevel systems, one need to make the assumption that the light-medium interaction is linear. In this case, all the previous calculations remain unchanged, but we need to change the expression for $\widetilde{\chi}(s)$ presented in (12). For instance, the susceptibility of the D_1 line of rubidium vapor will be as following:

$$\widetilde{\chi}(s) = \sum_{k=1}^{8} \langle \frac{iq_k}{su + \Gamma_k - i\Delta_k} \rangle_{u>0}, \tag{23}$$

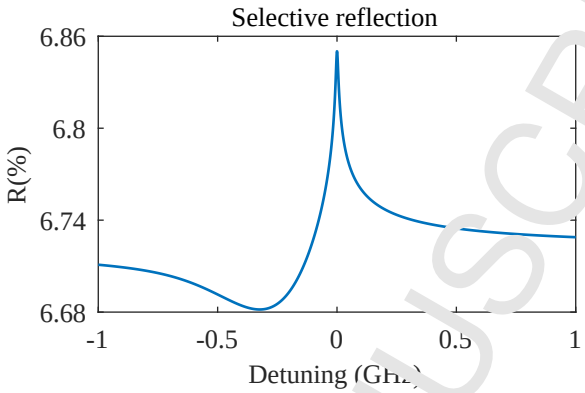

Figure 5: The selective reflection spectrum in the vicinity of the resonance line. The density of atoms is $N = 10^{13}\text{cm}^{-3}$.

where $q_k = N|d_k|^2/\hbar$ is a parameter, d_k are the dipole moments, $\Delta_k = \omega - \omega_k$ are the detunings from the corresponding resonance frequencies ω_k, Γ_k are the homogeneous widths of the corresponding $F \to F'$ hyperfine transitions for rubidium atomic vapor. The constants (e.g. dipole moment, resonance frequency) that we use here are taken from [38, 39]. The calculated spectrum of the rubidium D_1 line is shown in Fig.6.

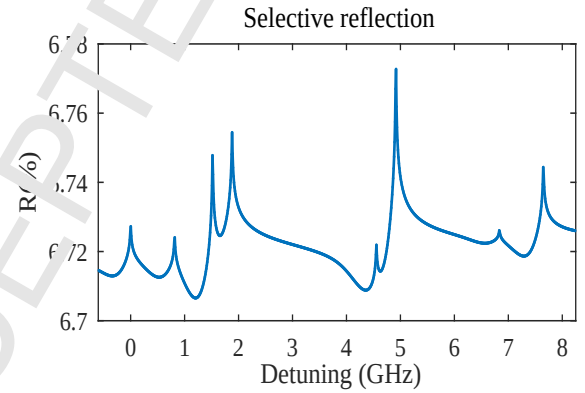

Figure 6: The selective reflection spectra from all Rb's D_1 lines (including both ^{85}Rb and ^{87}Rb). The density of atoms is $N = 10^{13}\text{cm}^{-3}$.

In Fig.6 we assume natural abundance for rubidium atoms (72.2% ^{85}Rb

and 27.8% ^{87}Rb). Here we also should mention that in (23) we don't take into account the depopulation of levels by assuming that it has a small effect on our model. The result can be compared to the experimental results obtained by Wang et al. [14] and Badalyan et al. [40] presented in the corresponding figures for rubidium D1 lines. Our result is consistent with the experimental curves presented there, although in these two papers the order of the density of the vapor is $N \approx 10^{14}\text{cm}^{-3}$.

Another interesting spectrum can be obtained by increasing the scale of detuning for the selective reflection. In this case we can see from Fig.7 that we have oscillations in the "wings" of the resonance line.

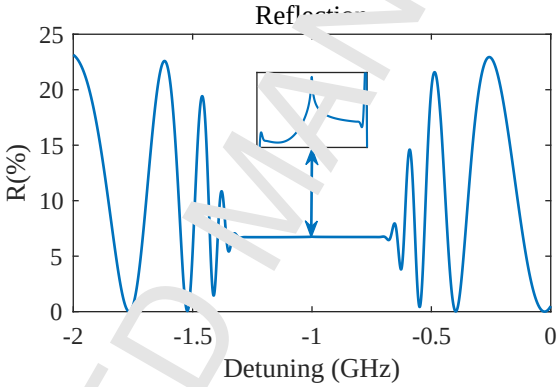

Figure 7: The multiple reflection spectrum from the Fabry-Perot interferometer in the far wings of the resonance line. In the insert we show the zoomed image of the horizontal line from the reflection spectrum. The density of atoms is $N = 3 \cdot 10^{13}\text{cm}^{-3}$.

In Fig.7 the selective reflection profile presented in Fig.5 also exists. Selective reflection profile is "hidden" in the region where we have a horizontal line in Fig.7. To see this one should zoom in this region and a picture like in Fig.5 will emerge (see the zoomed image). Fig.7 is interesting, because from this spectrum it is easy to straightforwardly obtain the group refractive index (see, for example [7]).

In regions near the resonance in Figs.5, 6 and in the horizontal region of Fig.7 we have only a single reflection from the first boundary. For the multiple reflection spectrum the light should be able to reach the second boundary, to reflect from it and, finally, to be able to reach and to pass the first boundary of the cell. If this doesn't happen, because the absorption is high in the vicinity

of the resonance line, there will be only a single reflection. To see a multiple reflection one should either decrease the length of the cell or decrease the density of the vapor. In Fig.8 we show the selective reflection from the cells with different lengths and fixed density $N = 10^{11}\text{cm}^{-3}$, calculated from (21).

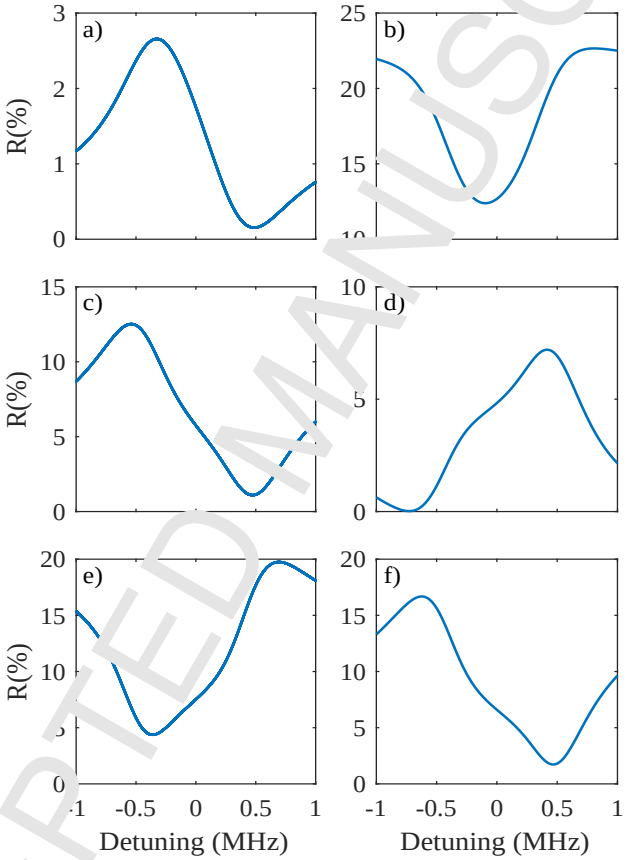

Figure 8: The selective reflection spectrum for different cell lengths. For subfigures a)-d) respectively cell lengths are $L = 0.2; 0.3; 0.6; 0.65; 0.7; 0.8\,\text{cm}$. The density of atoms is $N = 10^{11}\text{cm}^{-3}$.

In Fig.8 one can see different profiles of the selective reflection that correspond to different lengths of the medium. The differences arise from the fact that reflection is not generated from a single reflection, but from multiple reflections from the cell. Consequently, we will have interference picture due

to all these reflections. When we vary the length of the cell, the interference pattern changes and the profile of reflection also changes by its shape and amplitude.

6. Conclusion

In this paper we developed a self-consistent theory for the selective reflection from a dilute vapor. We determined formulas for single and multiple reflections. We obtained the spectrum for the effective refractive index that is also known as the surface admittance. Our results are well consistent with the above mentioned experimental results in the case of a dilute vapor. For a dense medium, we have to take into account effects like radiation trapping, the Dicke narrowing [41] etc.

Our developed model can be applied in a wide range of physical problems. For example, it can be used for determination of the density of unwanted (or desired) vapors by the selective reflection spectrum. If unwanted atoms have high enough density, the Fabry-Perot interferometer signal will be a single selective reflection that can be compared with the spectrum calculated from (22) and used to find the density of unwanted atoms. In the case when Fabry-Perot interferometer has a small length and the density of atoms is low enough that there will be multiple reflections from the boundaries of the cell, (21) can be used. Also, with this technique one can change the spectral profile of radiation by manipulating the length and the density of the dilute vapor cell, as presented in Fig.8. This theory can be generalized for multiphoton interactions that will provide an opportunity to address problems like, for example, selective reflection in EIT configuration [42].

Acknowledgments

The author is grateful to Gayane Grigoryan for stimulating discussions and valuable advices.

This work was supported by the RA MES State Committee of Science, in the frames of the research project no. 1-6/18A.

References

[1] Cojan, Jean-Louis, Contribution à l'étude de la réflexion sélective sur les vapeurs de mercure de la radiation de résonance du mercure, Ann.

Phys. 12 (9) (1954) 385–440. doi:10.1051/anphys/195412090385.
URL https://doi.org/10.1051/anphys/19541209038 5

[2] J. Woerdman, M. Schuurmans, Spectral narrowing of selective reflection from sodium vapour, Optics Communications 14 (2) (1975) 248 – 251. doi:https://doi.org/10.1016/0030-4018(75)90226-6.
URL http://www.sciencedirect.com/science/article/pii/0030401875902266

[3] Schuurmans, M. F. H., Spectral narrowing of selective reflection, J. Phys. France 37 (5) (1976) 469–485. doi:10.1051/jphys:01976003705046900.
URL https://doi.org/10.1051/jphys:01976003705046900

[4] E. A. Gazazyan, A. V. Papoyan, D. Sarkisyan, A. Weis, Laser frequency stabilization using selective reflection from a vapor cell with a half-wavelength thickness, Laser Physics Letters 4 (11) (2007) 801.
URL http://stacks.iop.org/1612-202X/4/i=11/a=002

[5] R. Li, S. Jia, D. Bloch, M. Ducloy, Frequency-stabilization of a diode laser with ultra-low power through linear selective reflection, Optics Communications 146 (1) (1998) 186 – 188. doi:https://doi.org/10.1016/S0030-4018(97)00478-1.
URL http://www.sciencedirect.com/science/article/pii/S0030401897004781

[6] R. Müller, A. Weis, Laser frequency stabilization using selective reflection spectroscopy, Applied Physics B 66 (3) (1998) 323–326. doi:10.1007/s003400050395.
URL https://doi.org/10.1007/s003400050395

[7] A. Papoyan, S. Shmavonyan, D. Khachatryan, G. Grigoryan, Straightforward retrieval of dispersion in a dense atomic vapor helped by buffer gas-assisted radiation channeling, J. Opt. Soc. Am. B 34 (4) (2017) 877–883. doi:10.1364/JOSAB.34.000877.
URL http://josab.osa.org/abstract.cfm?URI=josab-34-4-877

[8] L. Klinger, A. Sargsyan, C. Leroy, D. Sarkisyan, Selective reflection of laser radiation from submicron layers of Rb and Cs atomic vapors: Applications in atomic spectroscopy, Journal of Experimental and Theoretical Physics 125 (4) (2017) 543–550. doi:10.1134/S1063776117090151.
URL https://doi.org/10.1134/S1063776117090151

[9] A. Sargsyan, E. Klinger, Y. Pashayan-Leroy, C. Leroy, A. Papoyan, D. Sarkisyan, Selective reflection from Rb vapor in half- and quarter-wave cells: Features and possible applications, JETP Letters 104 (4) (2016) 224–230. doi:10.1134/S002136401616013X.
URL https://doi.org/10.1134/S002136401616013X

[10] H. Failache, S. Saltiel, M. Fichet, D. Bloch, M. Ducloy, Resonant coupling in the van der Waals interaction between an excited alkali atom and a dielectric surface: an experimental study via stepwise selective reflection spectroscopy, The European Physical Journal D - Atomic, Molecular, Optical and Plasma Physics 23 (2) (2003) 237–255. doi:10.1140/epjd/e2003-00098-4.
URL https://doi.org/10.1140/epjd/e2003-00098-4

[11] M. Fichet, G. Dutier, A. Yarovitski, P. Todorov, I. Hamdi, I. Maurin, S. Saltiel, D. Sarkisyan, M.-P. Gorza, D. Bloch, M. Ducloy, Exploring the van der Waals atom-surface attraction in the nanometric range, EPL (Europhysics Letters) 77 (3) (2007) 54001.
URL http://stacks.iop.org/0295-5075/77/i=5/a=54001

[12] A. Sargsyan, A. Papoyan, D. G. Hughes, C. S. Adams, D. Sarkisyan, Selective reflection from an Rb layer with a thickness below $\lambda/12$ and applications, Opt. Lett. 42 (8) (2017) 1476–1479. doi:10.1364/OL.42.001476.
URL http://ol.osa.org/abstract.cfm?URI=ol-42-8-1476

[13] V. Vuleti, V. Sautenkov, C. Zimmermann, T. Hnsch, Measurement of cesium resonance line self-broadening and shift with Doppler-free selective reflection spectroscopy, Optics Communications 99 (3) (1993) 185 – 190. doi:https://doi.org/10.1016/0030-4018(93)90076-H.
URL http://www.sciencedirect.com/science/article/pii/003040189390076H

[14] P. Wang, A. Gallagher, J. Cooper, Selective reflection by Rb, Phys. Rev. A 56 (1997) 1598–1606. doi:10.1103/PhysRevA.56.1598.
URL https://link.aps.org/doi/10.1103/PhysRevA.56.1598

[15] A. Papoyan, Measurement of collisional self broadening of atomic resonance lines in selective reflection experiment, J. Contemp. Phys. (Arm. Acad. Sci.) 33 (3) (1998) 109–114.
URL http://physics.asj-oa.am/id/eprint/816

[16] A. Papoyan, G. S. Sarkisyan, S. V. Shmavonyan, Selective reflection of light from dense sodium vapors, Optics and Spectroscopy 85 (1998) 649–652.

[17] B. Gross, N. Papageorgiou, V. Sautenkov, A. Weis, Velocity selective optical pumping and dark resonances in selective reflection spectroscopy, Phys. Rev. A 55 (1997) 2973–2981. doi:10.1103/PhysRevA.55.2973.
URL https://link.aps.org/doi/10.1103/PhysRevA.55.2973

[18] A. Weis, V. A. Sautenkov, T. W. Hänsch, Observation of ground-state Zeeman coherences in the selective reflection from cesium vapor, Phys. Rev. A 45 (1992) 7991–7996. doi:10.1103/PhysRevA.45.7991.
URL https://link.aps.org/doi/10.1103/PhysRevA.45.7991

[19] N. Papageorgiou, A. Weis, V. A. Sautenkov, D. Bloch, M. Ducloy, High-resolution selective reflection spectroscopy in intermediate magnetic fields, Applied Physics B 59 (2) (1994) 123–126. doi:10.1007/BF01081162.
URL https://doi.org/10.1007/BF01081162

[20] A. Sargsyan, E. Klinger, G. Hakhumyan, A. Tonoyan, A. Papoyan, C. Leroy, D. Sarkisyan, Decoupling of hyperfine structure of Cs D1 line in strong magnetic field studied by selective reflection from a nanocell, J. Opt. Soc. Am. B 34 (4) (2017) 776–784. doi:10.1364/JOSAB.34.000776.
URL http://josab.osa.org/abstract.cfm?URI=josab-34-4-776

[21] E. Klinger, A. Sargsyan, A. Tonoyan, G. Hakhumyan, A. Papoyan, C. Leroy, D. Sarkisyan, Magnetic field-induced modification of selection rules for Rb D2 line monitored by selective reflection from a vapor nanocell, The European Physical Journal D 71 (8) (2017) 216. doi:10.1140/epjd/e2017-80291-6.
URL https://doi.org/10.1140/epjd/e2017-80291-6

[22] A. Sargsyan, A. Tonoyan, J. Keaveney, I. G. Hughes, C. S. Adams, D. Sarkisyan, Selective reflection of potassium vapor nanolayers in a magnetic field, Journal of Experimental and Theoretical Physics 126 (3) (2018) 293–301. doi:10.1134/S106377611802005X.
URL https://doi.org/10.1134/S106377611802005X

[23] G. Nienhuis, F. Schuller, M. Ducloy, Nonlinear selective reflection from an atomic vapor at arbitrary incidence angle, Phys. Rev. A 38 (1988) 5197–5205. doi:10.1103/PhysRevA.38.5197.
URL https://link.aps.org/doi/10.1103/PhysRevA.38.5197

[24] M. Ducloy, M. Fichet, General theory of frequency modulated selective reflection. influence of atom surface interactions, J. Phys. II France 1 (12) (1991) 1429–1446. doi:10.1051/jp2:1991160.
URL https://doi.org/10.1051/jp2:1991160

[25] T. A. Vartanyan, A. Weis, Origin of the "blueshift" in selective reflection spectroscopy and its partial compensation by the local-field correction, Phys. Rev. A 63 (2001) 063813. doi:10.1103/PhysRevA.63.063813.
URL https://link.aps.org/doi/10.1103/PhysRevA.63.063813

[26] J. Guo, J. Cooper, A. Gallagher, M. Lewenstein, Theory of selective reflection spectroscopy, Optics Communications 110 (5) (1994) 732 – 743. doi:https://doi.org/10.1016/0030-4018(94)90279-8.
URL http://www.sciencedirect.com/science/article/pii/0030401894902798

[27] J. Guo, J. Cooper, A. Gallagher, Selective reflection from a dense atomic vapor, Phys. Rev. A 53 (1996) 1130–1138. doi:10.1103/PhysRevA.53.1130.
URL https://link.aps.org/doi/10.1103/PhysRevA.53.1130

[28] T. A. Vartanyan, D. L. Lin, Enhanced selective reflection from a thin layer of a dilute gaseous medium, Phys. Rev. A 51 (1995) 1959–1964. doi:10.1103/PhysRevA.51.1959.
URL https://link.aps.org/doi/10.1103/PhysRevA.51.1959

[29] B. Zambon, G. Nienhuis, Reflection and transmission of light by thin vapor layers, Optics Communications 143 (4) (1997) 308 – 314. doi:https://doi.org/10.1016/S0030-4018(97)00331-3.
URL http://www.sciencedirect.com/science/article/pii/S0030401897003313

[30] G. Dutier, S. Saltiel, D. Bloch, M. Ducloy, Revisiting optical spectroscopy in a thin vapor cell: mixing of reflection and transmission as a Fabry–Perot microcavity effect, J. Opt. Soc. Am. B 20 (5) (2003) 793–800. doi:10.1364/JOSAB.20.000793.
URL http://josab.osa.org/abstract.cfm?URI=josab-20-5-793

[31] A. L. J. Burgmans, M. F. H. Schuurmans, B. Bölger, Transient behavior of optically excited vapor atoms near a solid interface as observed in evanescent wave emission, Phys. Rev. A 16 (1977) 2002–2007. doi:10.1103/PhysRevA.16.2002.
URL https://link.aps.org/doi/10.1103/PhysRevA.16.2002

[32] V. Bordo, C. Henkel, A. Lindinger, H.-G. Rubahn, Evanescent wave fluorescence spectra of Na atoms, Optics Communications 137 (4) (1997) 249 – 253. doi:https://doi.org/10.1016/S0030-4018(97)00010-2.
URL http://www.sciencedirect.com/science/article/pii/S0030401897000102

[33] A. V. Papoyan, G. G. Grigoryan, S. V. Shmavonyan, D. Sarkisyan, J. Guéna, M. Lintz, M. A. Bouchiat, New feature in selective reflection with a highly parallel window: Phase-tunable homodyne detection of the radiated atomic field, The European Physical Journal D - Atomic, Molecular, Optical and Plasma Physics 30 (2) (2004) 265–273. doi:10.1140/epjd/e2004-00088-0.
URL https://doi.org/10.1140/epjd/e2004-00088-0

[34] O. Svelto, Principles of Lasers, 5th Edition, Springer US, 2010.

[35] M. H. Schuurmans, The fluorescence of atoms near a glass surface, Contemporary Physics 21 (5) (1980) 463–482. arXiv:https://doi.org/10.1080/00107518008210971, doi:10.1080/00107518008210971.
URL https://doi.org/10.1080/00107518008210971

[36] G. S. Landsberg, Optika (Optics), 6th Edition, Fizmatlit, 2003.

[37] D. Bloch, M. Ducloy, Atom-wall interaction, Vol. 50 of Advances In Atomic, Molecular, and Optical Physics, Academic Press, 2005, pp. 91 – 154. doi:https://doi.org/10.1016/S1049-250X(05)80008-4.
URL http://www.sciencedirect.com/science/article/pii/S1049250X05800084

[38] D. A. Steck, Rubidium 85 D line data (2013).
URL http://steck.us/alkalidata

[39] D. A. Steck, Rubidium 87 D line data (2015).
URL http://steck.us/alkalidata

[40] A. Badalyan, V. Chaltykyan, G. Grigoryan, A. Papoyan, S. Shmavonyan, M. Movsessian, Selective reflection by atomic vapor: experiments and self-consistent theory, The European Physical Journal D - Atomic, Molecular, Optical and Plasma Physics 37 (2) (2006) 157–162. doi:10.1140/epjd/e2005-00253-6.
URL https://doi.org/10.1140/epjd/e2005-00253-6

[41] R. H. Dicke, The effect of collisions upon the Doppler width of spectral lines, Phys. Rev. 89 (1953) 472–473. doi:10.1103/PhysRev.89.472.
URL https://link.aps.org/doi/10.1103/PhysRev.89.472

[42] M. Fleischhauer, A. Imamoglu, J. P. Marangos, Electromagnetically induced transparency: Optics in coherent media, Rev. Mod. Phys. 77 (2005) 633–673. doi:10.1103/RevModPhys.77.633.
URL https://link.aps.org/doi/10.1103/RevModPhys.77.633